Progress In Electromagnetics Research C, Vol. 109, 139–152, 2021

A Bidirectional LSTM-Based Prognostication of Electrolytic Capacitor

Delanyo K. B. Kulevome, Hong Wang*, and Xuegang Wang

Abstract—Knowing the state-of-health (SOH) of equipment, device or component is very essential for the secure and dependable operation of a system. Electrolytic capacitors are undoubtedly one of the essential components of power supply modules used in aerial and underwater vehicles, and every equipment requires a conversion of voltage from one level to another. This has encouraged research into the components of the power supply used in such systems of which electrolytic capacitor is of interest in this study. In this paper, we explore a new approach to implementing prognostics and health management (PHM) for electrolytic capacitors and propose a method of estimating the SOH leading to the prediction of the remaining useful life (RUL). This is accomplished by using a bidirectional long short-term memory (BLSTM) network to capture the degradation trends. We demonstrate the power and leverage that this method brings to bear in encoding time-domain dependencies in accurately estimating the SOH bereft of state models as employed in traditional methods. We validate the proposed approach using capacitor data recorded at different electrical over-stress accelerated aging conditions. The proposed method surpasses other existing methods in RUL prediction as indicated by the error and relative accuracy.

1. INTRODUCTION

Power supply modules are used in most equipment to provide power for functionality. This simple but important device has permeated every sector of our lives from household equipment to mission critical facilities. These modules serve as means of converting voltages and/or current from one DC level to another or from AC to DC. The electrolytic capacitors in providing smoothed output voltages tend to fail over the course of their operating life. These present unique challenges to performing root cause analysis when faults occur. However, since it is not practical to periodically interrupt the operation of an equipment to analyze and sample the state of health (SOH) of these devices, it is convenient to devise another approach to monitor the degeneration of these components and estimate the remaining useful life (RUL). Estimating the SOH is essential to safeguard the continual operation and establish confidence in the reliability of a system.

The concept of prognostics and health management (PHM) is based on the condition-based maintenance (CBM) approach. Incorporating the ability to perform estimations and predictions makes PHM an acceptable and reliable approach. The implementation of PHM can be dismembered into three activities. They are observing, analyzing, and decision making. PHM has been explored in several areas of engineering using physics-based models [1], data-driven models [2], or hybrid models [3]. In capacitor health management, the empirical model is used in estimating the end of life (EOL) and predicting the RUL. The problem of estimating the RUL under variable operating condition of a capacitor is investigated by Rigamonti et al. [4], and a physics based model is developed in a particle filter framework

Received 2 December 2020, Accepted 26 January 2021, Scheduled 3 February 2021
* Corresponding author: Hong Wang (hongw@uestc.edu.cn).
The authors are with the School of Information and Communication Engineering, University of Electronic Science and Technology of China, Sichuan, Chengdu, P. R. China.

to predict the RUL of an electrolytic capacitor. In like fashion, Celaya et al. [5] proposed an empirical model in the Kalman filter framework to predict the RUL of electrolytic capacitors with reasonable performance. However, their model failed to capture the change in the behavior of the degradation trend toward the end of the test data. An analysis of the degeneration in electrolytic capacitors was studied by Renwick et al. [6] under electrical over-stress by measuring the rise time (τ) during each cycle. Jamshidi and Alibeigi [7] investigated a soft computing approach for RUL estimation of electrolytic capacitors using an adaptive neuro fuzzy inference system (ANFIS). A simple and cost-effective approach was conducted to monitor the condition of the DC-Link capacitors in adjustable speed drives [8]. Qin et al. [9] proposed a method to automatically estimate the capacitance and equivalent series resistance (ESR) of a capacitor in an environment free of noise as well as independent of the variations in the temperature or load. The approaches adopted by the aforementioned papers had some challenges and could not adapt well to the degradation trend which was equally identified in [9]. The exponential model is common in the implementation of an empirical model. However, its simplistic nature fails to capture the degradation trend accurately. Therefore, an adaptive method [9] using an empirical model is achieved through the combination of two models. This method has also left a gap as it also relies on the use of empirical models in predicting the RUL.

In recent times, deep learning methods have been applied in diverse applications [10–12] with significant amount of success. This has inspired researchers to gravitate towards applying relevant deep learning approaches in PHM implementations [13, 14].

In this research paper, we propose a bidirectional long short-term memory (BLSTM) based prognostics model which is a variant of the recurrent neural network (RNN) to estimate the SOH through the prediction of the percentage decrease in capacitance. Our contributions in this research are given as follows:

(i) Motivated by the fact that little research has been undertaken in applying deep learning methods to capacitance health prediction, we implement multilayer perceptron (MLP) and Long Short-Term Memory (LSTM) models to compare with the performance of the proposed model.

(ii) We leverage the ability of the BLSTM to learn its own parameters through back propagation through time (BPTT) in training the degradation data samples. This is contrary to the physics-based or model-based methods using lumped parameters and equivalent circuits to model the internal characteristics of the capacitor which require much time to parameterize.

(iii) We implement a BLSTM network to efficiently relate the matrix of features to the SOH of the capacitors directly without the need for state space equations and inference algorithms used in particle filters, Kalman filters, and other variants.

The effectiveness of the proposed method is verified using the standard capacitor dataset available at the NASA dataset repository [6]. The rest of the paper is organized as follows: Section 2 describes the fundamental principles of PHM. Section 3 investigates and analyzes the mechanisms that cause failure in electrolytic capacitors. Section 4 expounds on the overview of the proposed model and the process used in undertaking this research. Section 5 presents the BLSTM based health monitoring and prognostics of electrolytic capacitors. In Section 6, the results are presented and discussed. The conclusion is drawn in Section 7.

2. FUNDAMENTAL PRINCIPLES OF PHM

Prognostics is an essential component in data-driven process for PHM. This begins with the collection and observation of operational history of a device. An unusual behavior in the data is an indication of a potential failure warning. Diagnosis is then performed to extract the information relating to the identified anomaly in the data [15, 16]. This information, in addition to other relevant historical and operational details, is used in the prognostics to estimate the RUL, and appropriate measures are taken based on the outcome [17]. The constituents of a PHM framework is illustrated in Figure 1(a). An exemplary behavior in the possible operating pattern of a typical system is shown in Figure 1(b) which highlights a normal and degraded performance region.

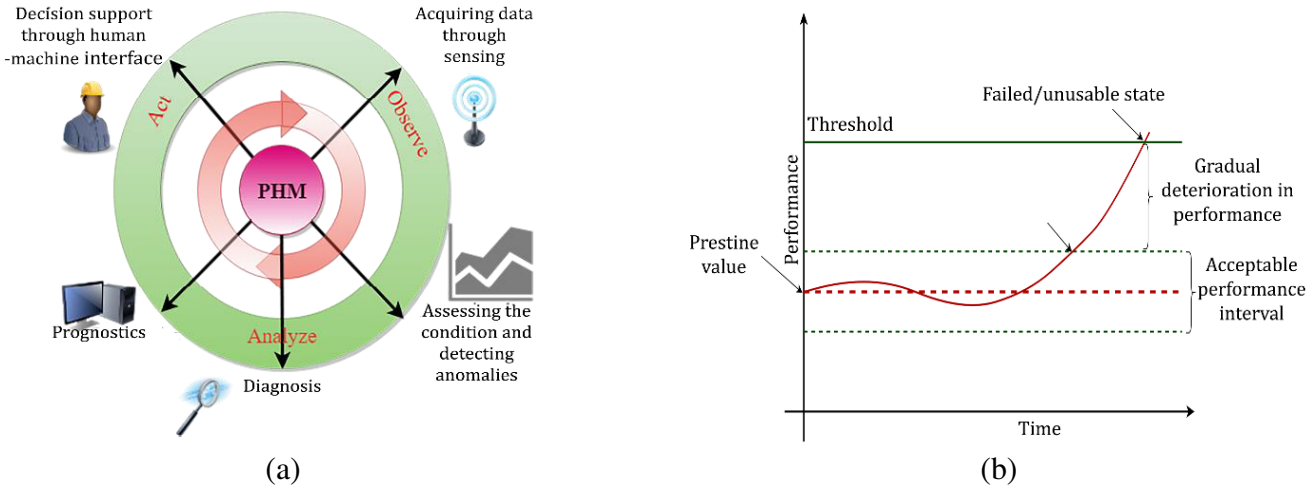

Figure 1. (a) Constituents of a PHM framework, (b) typical degradation in performance.

3. ELECTROLYTIC CAPACITOR

The simplest representation of a capacitor is two parallel plates separated by a dielectric material having uniform thickness. The external connection is made up of a positive and negative electrode having good electrical conductivity. When a voltage source is connected across its terminals, electrical charges are induced in the dielectric material. The permittivity of this dielectric material in addition to the distance between the parallel plates and area determines the overall capacitance value. However, an in-depth analysis of an electrolytic capacitor shows that it comprises an anode foil covered with thin dielectric layer (Aluminum Oxide) interleaved with paper and impregnated in an electrolyte as shown in Figure 2.

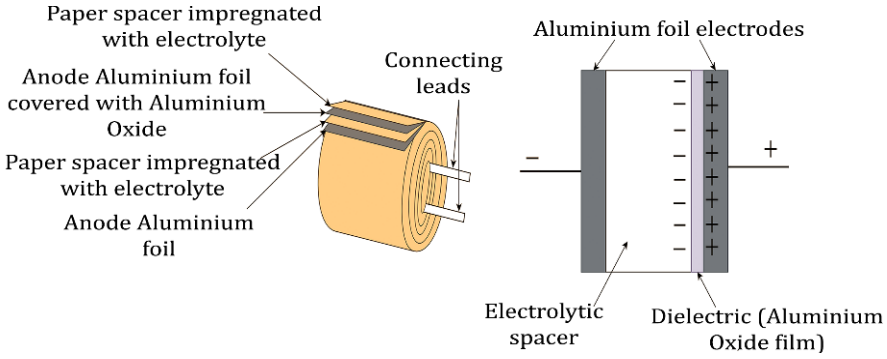

Figure 2. Structure of an electrolytic capacitor.

3.1. Degeneration and Failure Mechanisms in an Electrolytic Capacitor

The ESR of the capacitor is the combination of the ohmic (R_o), frequency dependent dielectric layer (R_d), and temperature dependent (R_e) resistances. The propensity of an electrolytic capacitor in a device to fail has been rated around 60% as compared to other components under rated conditions at an operating temperature of 25°C [18] as given in Figure 3(a). The conditions under which a capacitor operates can significantly affect its performance. The electrolyte impregnated in an aluminum electrolytic capacitor vaporizes over time and leads to the deterioration of the capacitor [5]. Some prominent factors that can contribute to the degradation of the capacitor over its useful life are illustrated in Figure 3(b).

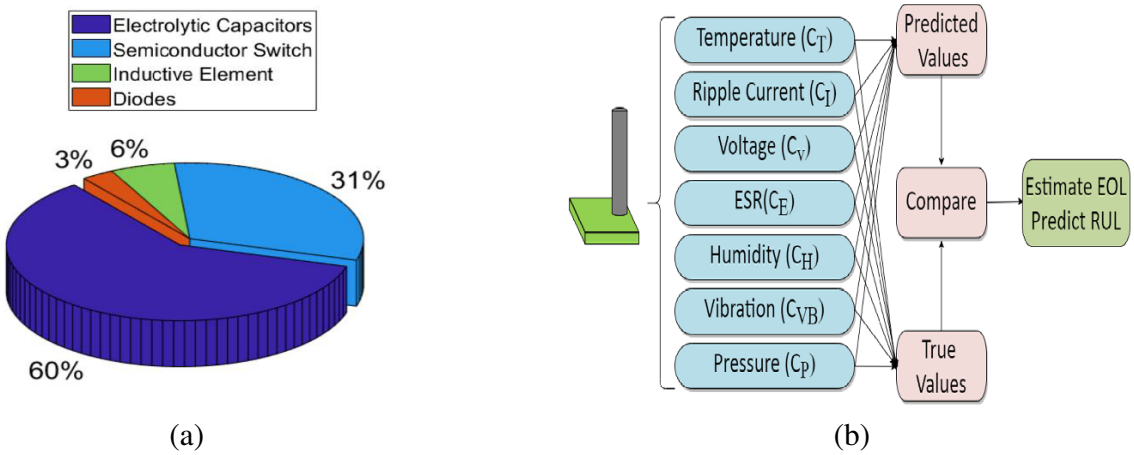

Figure 3. (a) Probability of failure of components in a device, (b) factors that can contribute to the degradation of an electrolytic capacitor.

3.1.1. Effect of Temperature

Within an aluminum electrolytic capacitor, the rise in temperature and power dissipation are directly proportional [19] and occur when the voltage across the dielectric material varies. The efficient operation of the capacitor is highly dependent on the ambient temperature. Wide variations of the internal and external temperatures can affect its stipulated performance. High temperatures within the capacitor result in the evaporation of the electrolyte leading to its degradation. Leakage current also contributes to heat accumulation within the capacitor capsule [20].

3.1.2. Effect of Pressure

The diminishing rate of the electrolyte has a direct relationship with the electrolyte vapor pressure as a result of internal chemical reaction and rise in temperature which occurs due to the charge and discharge cycles [19].

3.1.3. Effect of Voltage

The voltage range within which the capacitor operates is one of the important characteristics that must be considered. High operating voltages applied to the terminals of an electrolytic capacitor will eventually lead to the degradation and potential destruction of a capacitor.

3.1.4. Effect of Ripple Current

The ripple current contributes to power dissipation and self-heating within the capacitor which results in temperature rise. High levels of ripple current will eventually reduce the reliability of a capacitor in a circuit.

3.1.5. Effect of ESR

Increase in ESR arises as a result of depreciation in the electrolyte volume which in turn decreases the capacitance. As this occurs, there is a cumulative rise in temperature which aggravates the electrolyte evaporation process [21]. Also, the variation in ESR is frequency dependent, and it is inversely proportional to the temperature.

3.1.6. Effect of Humidity

The ingress and accumulation of moisture results from temperature variations which can cause corrosion of the capacitor electrodes. When being taken into account, it can have a slight influence on the degradation of a capacitor.

3.1.7. Effect of Vibration

Under normal conditions, minor vibrations should not affect the performance or life of an electrolytic capacitor. However, under excessive vibration environments, the connecting leads may get detached and lose contact with the remaining circuitry. Under worse conditions, the life of the capacitor can be drastically shortened leading to catastrophic failure.

The interaction of diverse factors can affect the performance and life of electrolytic capacitors as aforementioned. From the preceding analysis and juxtaposing the various effects, it can be realized that two major factors stand out. These are the temperature and ESR whose effect on the life of electrolytic capacitor is influenced by the remaining other factors.

We proceed by building a BLSTM architecture to predict and estimate the EOL and RUL of electrolytic capacitor under accelerated electrical over-stress aging condition.

4. OVERVIEW OF PROPOSED METHOD

The LSTM network is an improvement on the RNN by introducing memory cells to overcome the vanishing and exploding gradient problem inherent in classical RNNs [22, 23]. We therefore capitalize on the learning function of LSTM to model the temporal dynamics of sampled data in prognostics scenarios. However, to make the learning process more efficient, we adopt the BLSTM which is composed of two parallel layers propagating in both the forward and backward directions of each hidden layer [24]. By doing so, the pattern in the actual data can be captured in both the past and future contexts which is gainful in sequential learning [25]. The degradation in the capacitance value can be observed as time series data over a given period of time. For this reason, the BLSTM network is used to learn the pattern in the degradation data to estimate the SOH and predict the RUL and EOL.

4.1. Problem Representation

We begin our study by considering six electrolytic capacitors whose health conditions have been monitored and stored over a given time. Therefore, the actual RUL and EOL can be inferred during training. However, extrapolation from a given point in time to the EOL is estimated by the model. A perfect match between given points is highly desirable, hence the best achievable results must be the closest predictions to actual values. The objective is to find the mapping between the true and estimated values so as to minimize the error. The training of deep networks can be propounded as a non-convex optimization problem [26].

4.2. The Architecture of BLSTM

As aforementioned, the BLSTM is composed of two parallel layers of LSTM networks propagating in the forward and backward directions. The architecture of a BLSTM is shown in Figure 4.

The activation functions used in the realization of the LSTM network are the sigmoid function (σ) and the hyperbolic tangent function (tanh) given by:

$$\begin{aligned} \sigma(z) &= \left(\frac{1}{1+e^{-z}}\right) \\ \tanh(z) &= \frac{e^{z}-e^{-z}}{e^{z}+e^{-z}} \end{aligned} \tag{1}$$

The initial stage of the LSTM is the decision to retain or discard information and pass the outcome to the cell state. The sigmoid function transforms the output of the forget gate to lie between 0 and

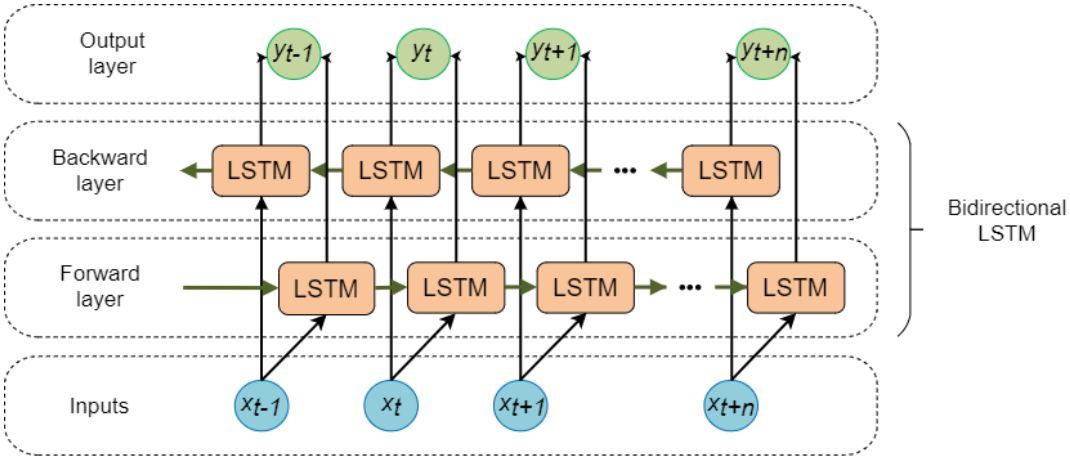

Figure 4. Illustration of BLSTM architecture.

1. The complete retention of information is represented by 1 whereas 0 denotes a complete removal of information [27]. This is given by:

$$f_t = \sigma(\theta_{xf} x_{(t)} + \theta_{hf} h_{t-1} + b_f) \tag{2}$$

where f_t is the forget gate, b_f the bias term, and θ the layer weights.

The input gate (i_t) and input node (g_t) select the amount of new computed information to be stored in the internal state. These are computed as:

$$i_t = \sigma(\theta_{xi} x_{(t)} + \theta_{hi} h_{(t-1)} + b_i) \tag{3}$$

$$g_t = \tanh(\theta_{xg} x_{(t)} + \theta_{hg} h_{(t-1)} + b_g) \tag{4}$$

The updated cell state C_t at time t is a combination of Eqs. (2)–(4) expressed as:

$$C_{(t)} = (f_t \odot C_{(t-1)}) \oplus (i_t \odot g_t) \tag{5}$$

The output gate (o_t) determines how much information in the internal state moves on to the next layer.

$$o_t = \sigma(\theta_{xo} x_{(t)} + \theta_{ho} h_{(t-1)} + b_o) \tag{6}$$

$$h_{(t)} = o_t \odot \tanh(C_{(t)}) \tag{7}$$

Since BLSTM has two LSTM layers, there are forward and backward passes which result in two outputs given by:

$$hf_t = H(\theta_{xhf} x_t + \theta_{hfhf} hf_{t-1} + b_{hf}) \tag{8}$$

$$hb_t = H(\theta_{xhb} x_t + \theta_{hbhb} hb_{t-1} + b_{hb}) \tag{9}$$

where hf and hb are the outputs of the forward and backward layers, respectively.

4.3. Training the Model

The main idea behind the training process of the network is to find the best parameters in order to minimize the loss function. The LSTM is modeled around three layers. They are the input, hidden, and output layers sequentially. In the proposed model, the inputs are passed into the BLSTM network, and the output features are computed. The element-wise summation of the forward and backward pass of each time-step results in the total output feature given by:

$$h_t^{(1)} = hf_t^{(1)} \oplus hb_t^{(1)} \tag{10}$$

A fully connected layer transforms the final hidden state tensor hF_t into a single SOH estimated value at time-step t through a rectified linear unit $g(\cdot)$ as follows:

$$\hat{SOH}_t = g(F_{out} hF_t + b_z) \tag{11}$$

where F_{out} and b_z represent the weight matrix of the fully connected layer and the biases, respectively.

In this paper, mean squared error (MSE) is used as the function for computing the loss. The discrepancy between the actual and estimated SOHs at each time step is expressed as:

$$L = \sum_{n=1}^{N} \left[\frac{1}{N} \left(SOH^{(n)} - \hat{SOH}^{(n)} \right)^2 \right] \tag{12}$$

where N is the total training set, and the actual and estimated SOH values in the training set are $SOH^{(n)}$ and $\hat{SOH}^{(n)}$, respectively.

To overcome the problem of over fitting, the dropout regularization [28] is used to modify the network itself rather than adjusting the cost function by randomly dropping a given percentage of total neurons in a layer in addition to all the connections to and from these neurons during each training iteration. The 'thinned' neurons comprises all the neurons that remained after the dropout as shown in Figure 5.

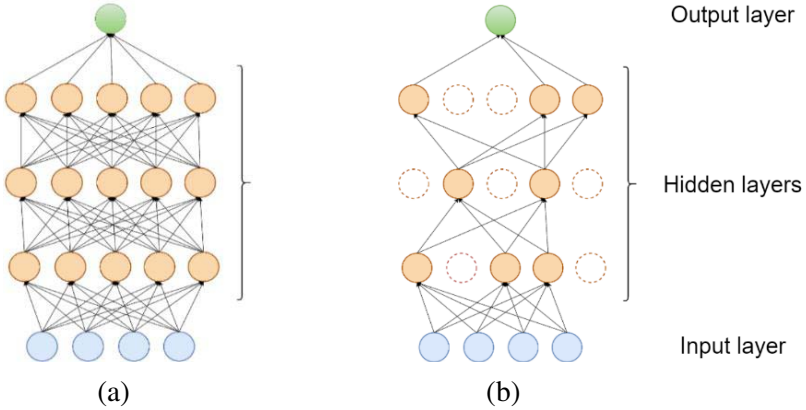

Figure 5. Dropout regularization, (a) no dropout, (b) dropout.

This culminates in a revamped network capable of generalizing better. The Adaptive Moment Estimation (Adam) Optimizer is chosen in building the model due to its effectiveness in improving the learning process [29].

4.4. Data Preparation

The dataset acquired is preprocessed prior to implementation by sampling points from each of the six original datasets to enhance training and offer better prediction. The min-max normalization is used to scale the data to range from 0 to 1.

$$x_{\text{norm}}^{(i)} = \frac{x^{(i)} - x_{\min}}{x_{\max} - x_{\min}} \tag{13}$$

where $x^{(i)}$ is the ith sample, and $x_{\min}$ and $x_{\max}$ are the minimum and maximum values in the feature columns, respectively.

4.5. Model Evaluation

The veracity of the proposed approach is evaluated using the mean absolute percentage error (MAPE), root mean square error (RMSE), and the relative accuracy (RA) at different prediction start times expressed as:

$$\text{RMSE} = \sqrt{\frac{\sum_{t=1}^{n} (SOH_t - \hat{SOH}_t)^2}{n}} \tag{14}$$

$$\text{MAPE} = \frac{100}{n}\sum_{t=1}^{n}\left|\frac{SOH_t - \hat{SOH}_t}{SOH_t}\right| \tag{15}$$

where SOH_t, $\hat{SOH}_t$, and n are the actual, predicted, and number of sample values, respectively.

$$\text{RA} = 1 - \frac{|\text{Actual}_{\text{RUL}} - \text{Predicted}_{\text{RUL}}|}{\text{Actual}_{\text{RUL}}} \tag{16}$$

5. EXPERIMENTAL ESTIMATION OF CAPACITANCE DEGENERATION

The capacitor dataset is acquired from NASA data repository. This includes the percentage decrease in the capacitance of six electrolytic capacitors which are subjected to electrical over-stress under accelerated aging condition as indicated in Figure 6. The mean capacitance of these capacitors is 2123 µF. The experimental details of the accelerated electrical over-stress aging of these capacitance are expounded in [30].

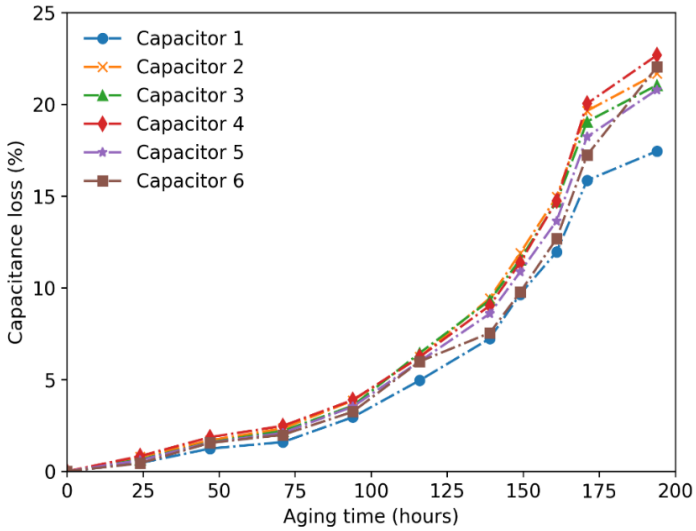

Figure 6. The percentage loss in capacitance [31].

Prior to training the proposed BLSTM based model, a given percentage of the dataset is reshaped into the required form using a sliding time window (TW) technique. This makes the network observe a given number of capacitor values up to a given time (t) and predict the next output at time ($t+1$) based on the captured trend.

The experiments are conducted using the proposed model to perform estimations and predictions based on observed data, and its performance is compared to MLP and LSTM models. These are performed on an Intel Core i5 laptop equipped with 8 GB RAM. The operating system is windows 10, and python 3.6 is the programming language used in formulating the models with Keras API [32]. The overall process of implementing the proposed model is illustrated in Figure 7.

To select the best hyperparameters for training, a random search is performed for the number of units, number of layers, dropout, batch size, and the number of epochs. The extremities of these hyperparameters are set to [1, 1, 0.0, 2, 20] and [200, 5, 0.5, 12, 200] with step size of [5, 1, 0.1, 2, 20]. Table 1 shows the best parameters for BLSTM for the six capacitors under various training datasets. Twenty experimental trials are conducted with the optimal hyperparameters, and the average performance is recorded. The choice of hyperparameter configuration plays a vital role in the performance of a model, and as such, the impact of the sliding TW length on the RUL prediction is also investigated.

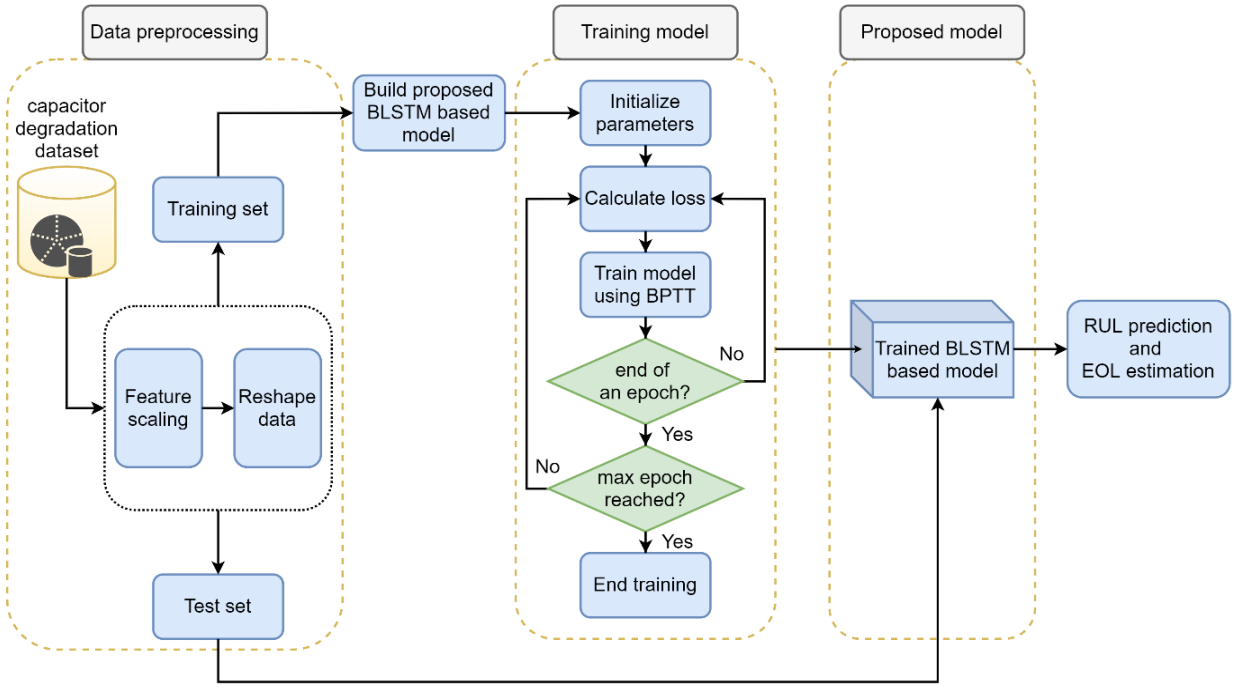

Figure 7. Flowchart of the proposed method for EOL estimation and RUL prediction.

Table 1. Optimal parameters for BLSTM models.

Training data	Batch size	Epoch	Units	Dropout
0–60	8	120	136	0.2
0–80	6	120	131	0.1
0–100	4	140	96	0.0
0–120	6	100	86	0.0

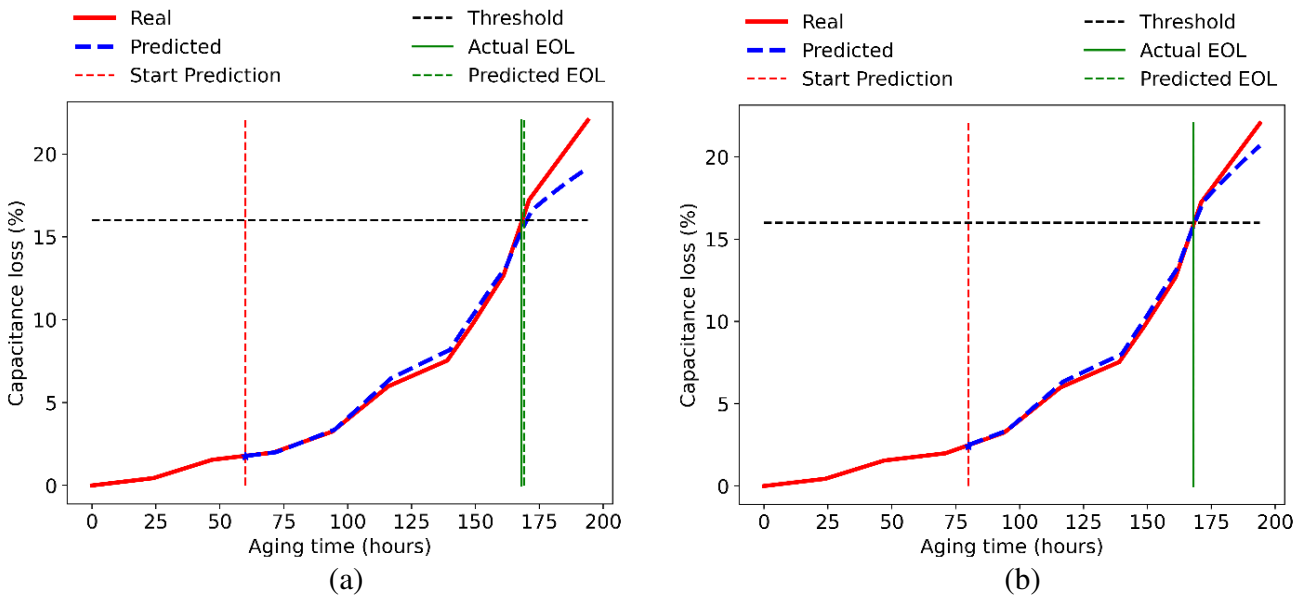

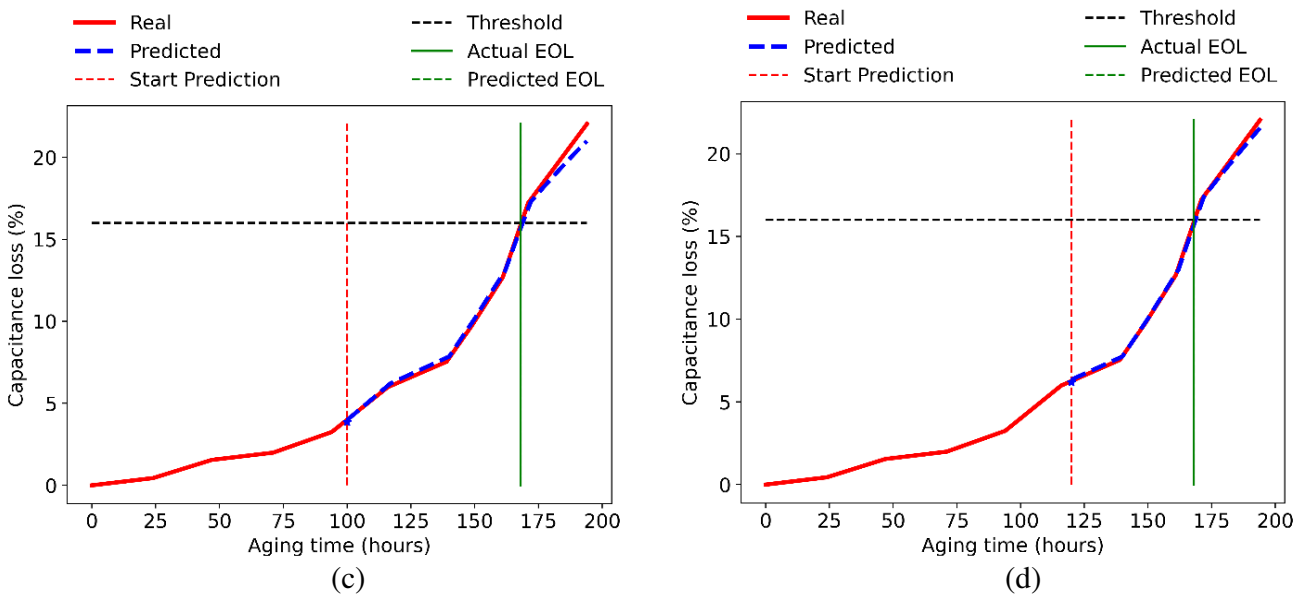

Figure 8. Prediction results of capacitor #6 using proposed BLSTM-based approach, (a) prediction from $t = 60$, (b) prediction from $t = 80$, (c) prediction from $t = 100$, (d) prediction from $t = 120$.

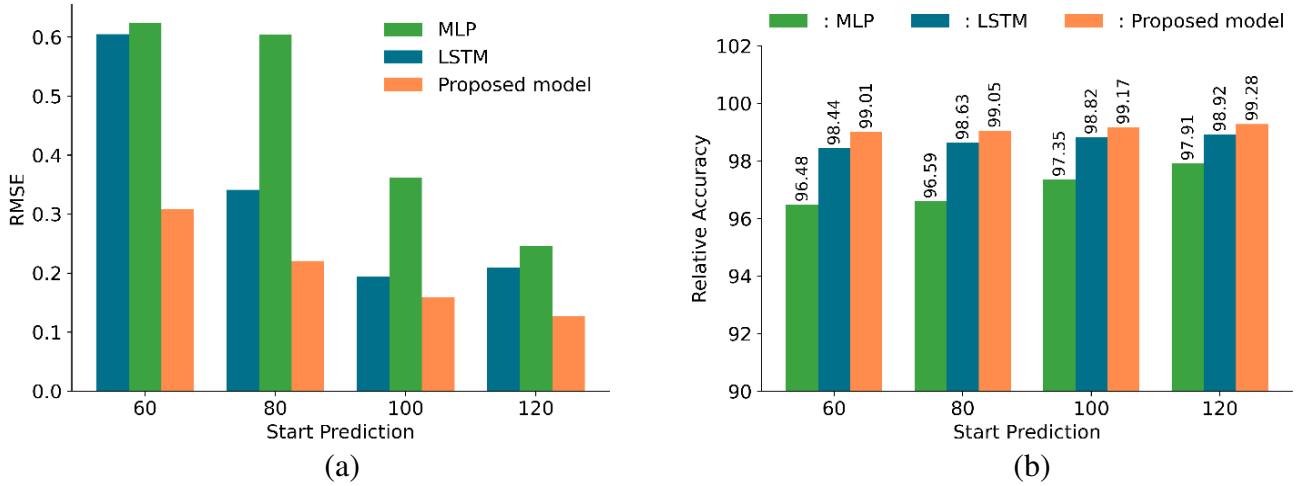

Figure 9. (a) RMSE comparison of predictions, (b) relative accuracy of predicted results.

6. RESULTS AND DISCUSSION

The requirement for establishing the inefficacy of a capacitor is outlined in [5]. Under electrical operations, a capacitor is deemed to have failed if its value decreases by 20% of its pristine value. However, in this study, a threshold value of 16% is set, and prediction start times of 60th, 80th, 100th, and 120th hour are selected. After training and testing the proposed BLSTM network with the preprocessed dataset, the average prediction results of capacitor #6 at selected times are shown in Figure 8. It can be observed that the proposed model performs creditably in estimating the RUL and predicting the EOL of the degrading capacitors.

It can be seen from the results that the actual EOL is at 168, and the mean EOL is predicted by the proposed model at various prediction start points. Setting $t = 60$, the actual RUL is 108 hours, and the EOL predicted by the model is 169. This results in a predicted RUL of 109 hours. The discrepancy in

Table 2. Comparing model performance under varied starting points for capacitor #6.

Models	Start Prediction	Actual EOL	Predicted EOL	Actual RUL	Predicted RUL	RA (%)	RMSE	MAPE
MLP	60th	168	172	108	112	96.48	0.6237	6.4242
	80th	168	171	88	91	96.59	0.6038	5.9892
	100th	168	170	68	70	97.35	0.3614	2.7829
	120th	168	170	48	50	97.91	0.2466	1.6257
LSTM	60th	168	167	108	107	98.44	0.6050	7.133
	80th	168	167	88	87	98.63	0.3414	3.8014
	100th	168	169	68	69	98.82	0.1943	2.0281
	120th	168	167	48	47	98.92	0.2092	2.1420
Proposed BLSTM based model	60th	168	169	108	109	99.01	0.3083	3.5096
	80th	168	168	88	88	99.05	0.2206	2.3819
	100th	168	168	68	68	99.17	0.1594	1.8421
	120th	168	168	48	48	99.28	0.1268	1.4465

Table 3. Average prediction performance of capacitor 1–5.

Dataset	Start Prediction	Actual EOL	Predicted EOL	Actual RUL	Predicted RUL	RMSE	MAPE (%)
Capacitor 1	60	171	172	111	112	0.4847	6.7973
	80	171	172	91	92	0.2554	2.9824
	100	171	171	71	71	0.1482	1.8746
	120	171	171	51	51	0.1178	1.1792
Capacitor 2	60	163	161	103	101	0.5075	4.2115
	80	163	163	83	83	0.1842	2.5436
	100	163	163	63	63	0.1780	1.9546
	120	163	163	43	43	0.0533	0.7428
Capacitor 3	60	163	164	103	104	0.3349	3.4325
	80	163	164	83	84	0.1744	2.1915
	100	163	163	63	63	0.1660	1.2788
	120	163	163	43	43	0.1592	1.3106
Capacitor 4	60	163	162	103	102	0.4546	4.9643
	80	163	164	83	84	0.1329	2.1768
	100	163	163	63	63	0.1169	2.0907
	120	163	163	43	43	0.0744	1.1577
Capacitor 5	60	166	167	106	107	0.3673	3.7725
	80	166	167	86	87	0.1565	1.5933
	100	166	165	66	65	0.1646	1.4309
	120	166	166	46	46	0.0871	0.9187

prediction by the model is computed by taking the difference between the actual and predicted results. This same analysis is performed on prediction start time of $t = 80$, 100, 120 consecutively. It can be inferred from the final analysis that satisfactory RUL predictions are produced as more data become available for training in terms of the prediction start time. Since the BLSTM can access both previous and future information, it greatly improves the training ability hence giving it an edge over the other methods as shown in Figure 9. To validate the veracity of the proposed model, its performance is measured against MLP and LSTM models as reported in Table 2.

To substantiate the efficacy of the proposed model holistically, further experiments were conducted on the remaining five capacitor degradation dataset, and the performance of the proposed method in predicting the RUL at selected times is presented in Table 3. This leads to the conclusion that the proposed approached has the ability to generalize well towards the EOL and RUL prediction of electrolytic capacitors under electrical over-stress conditions. From Table 3, it can be observed that the 60th hour prediction start point records high values of RMSE, and hence the predicted RUL slightly deviates from the true value. This is attributed to the limited training data available prior to this point.

7. CONCLUSION

In this research study, a model based on BLSTM network for the prognostics and health monitoring of electrolytic capacitors was proposed for an equitable RUL prediction. Noteworthy attributes of the proposed approach include leveraging the learning and memory retention capability of the BLSTM networks through self-learning even when samples in each training set were limited. Even though the other methods performed equally well, the proposed method produced meticulous predictions of the RUL with minimal errors. This approach has proven to be a promising method for capacitance performance over a period of time and sets the pace for future diagnostics and prognostics strategies. There are still more opportunities for improvement in this area. Therefore, in future studies, we will consider multiple operating conditions and characteristics of the electrolytic capacitor in determining its performance and predicting the RUL.

ACKNOWLEDGMENT

This work was supported by the National Aeronautical Fund (No. ASFC-20172080005).

REFERENCES

1. Downey, A., Y.-H. Lui, C. Hu, S. Laflamme, and S. Hu, "Physics-based prognostics of lithium-ion battery using non-linear least squares with dynamic bounds," *Reliab. Eng. Syst. Saf.*, Vol. 182, 1–12, 2019.
2. Xia, M., X. Zheng, M. Imran, and M. Shoaib, "Data-driven prognosis method using hybrid deep recurrent neural network," *Appl. Soft Comput.*, Vol. 93, 106351, 2020.
3. Du, P., J. Wang, W. Yang, and T. Niu, "A novel hybrid model for short-term wind power forecasting," *Appl. Soft Comput.*, Vol. 80, 93–106, 2019.
4. Rigamonti, M., P. Baraldi, E. Zio, D. Astigarraga, and A. Galarza, "Particle filter-based prognostics for an electrolytic capacitor working in variable operating conditions," *IEEE Trans. Power Electron.*, Vol. 31, No. 2, 1567–1575, 2015.
5. Celaya, J. R., C. S. Kulkarni, S. Saha, G. Biswas, and K. Goebel, "Accelerated aging in electrolytic capacitors for prognostics," *Proceedings of the Annual Reliability and Maintainability Symposium*, 1–6, 2012.
6. Renwick, J., C. S. Kulkarni, and J. R. Celaya, "Analysis of electrolytic capacitor degradation under electrical overstress for prognostic studies," *Proceedings of the Annual Conference of the Prognostics and Health Management Society*, Vol. 6, 2015.
7. Jamshidi, M. B. and N. Alibeigi, "Neuro-fuzzy system identification for remaining useful life of electrolytic capacitors," *2017 2nd International Conference on System Reliability and Safety (ICSRS)*, 227–231, 2017.

8. Lee, K.-W., M. Kim, J. Yoon, S. Bin Lee, and J.-Y. Yoo, "Condition monitoring of DC-link electrolytic capacitors in adjustable-speed drives," *IEEE Trans. Ind. Appl.*, Vol. 44, No. 5, 1606–1613, 2008.
9. Qin, Q., S. Zhao, S. Chen, D. Huang, and J. Liang, "Adaptive and robust prediction for the remaining useful life of electrolytic capacitors," *Microelectron. Reliab.*, Vol. 87, 64–74, 2018.
10. Garcia-Garcia, A., S. Orts-Escolano, S. Oprea, V. Villena-Martinez, P. Martinez-Gonzalez, and J. Garcia-Rodriguez, "A survey on deep learning techniques for image and video semantic segmentation," *Appl. Soft Comput.*, Vol. 70, 41–65, 2018.
11. Chen, X., Z. Wei, M. Li, and P. Rocca, "A review of deep learning approaches for inverse scattering problems (invited review)," *Progress In Electromagnetics Research*, Vol. 167, 67–81, 2020.
12. Liu, C., M.-H. Yang, and X.-W. Sun, "Towards robust human millimeter wave imaging inspection system in real time with deep learning," *Progress In Electromagnetics Research*, Vol. 161, 87–100, 2018.
13. Lin, Y., X. Li, and Y. Hu, "Deep diagnostics and prognostics: An integrated hierarchical learning framework in PHM applications," *Appl. Soft Comput.*, Vol. 72, 555–564, 2018.
14. Zhang, L., J. Lin, B. Liu, Z. Zhang, X. Yan, and M. Wei, "A review on deep learning applications in prognostics and health management," *IEEE Access*, Vol. 7, 162415–162438, 2019.
15. Cabanas, M. F., F. Pedrayes González, M. G. Melero, C. H. Rojas García, G. A. Orcajo, J. M. Cano Rodríguez, and J. G. Norniella, "Insulation fault diagnosis in high voltage power transformers by means of leakage flux analysis," *Progress In Electromagnetics Research*, Vol. 114, 211–234, 2011.
16. Faiz, J. and B. M. Ebrahimi, "Mixed fault diagnosis in three-phase squirrel-cage induction motor using analysis of air-gap magnetic field," *Progress In Electromagnetics Research*, Vol. 64, 239–255, 2006.
17. Vasan, A. S. S., B. Long, and M. Pecht, "Diagnostics and prognostics method for analog electronic circuits," *IEEE Trans. Ind. Electron.*, Vol. 60, No. 11, 5277–5291, 2012.
18. Venet, P., F. Perisse, M. H. El-Husseini, and G. Rojat, "Realization of a smart electrolytic capacitor circuit," *IEEE Ind. Appl. Mag.*, Vol. 8, No. 1, 16–20, 2002.
19. Kulkarni, C., G. Biswas, J. Celaya, and K. Goebel, "Prognostic techniques for capacitor degradation and health monitoring," *The Maintenance & Reliability Conference, MARCON*, 2011.
20. Gupta, A., O. P. Yadav, D. DeVoto, and J. Major, "A review of degradation behavior and modeling of capacitors," *ASME 2018 International Technical Conference and Exhibition on Packaging and Integration of Electronic and Photonic Microsystems*, Vol. 51920, 2018.
21. Leite, A. V. T., H. J. A. Teixeira, A. J. Marques Cardoso, and R. M. Esteves Araujo, "A simple ESR identification methodology for electrolytic capacitors condition monitoring," *Proceedings of the 20th International Congress on Condition Monitoring and Diagnostic Engineering Management, COMADEM'07*, 75–84, 2007.
22. Hochreiter, S. and J. Schmidhuber, "Long short-term memory," *Neural Comput.*, Vol. 9, No. 8, 1735–1780, 1997.
23. Pascanu, R., T. Mikolov, and Y. Bengio, "On the difficulty of training recurrent neural networks," *International Conference on Machine Learning*, 1310–1318, 2013.
24. Huang, C.-G., H.-Z. Huang, and Y.-F. Li, "A bidirectional LSTM prognostics method under multiple operational conditions," *IEEE Trans. Ind. Electron.*, Vol. 66, No. 11, 8792–8802, 2019.
25. Huang, C.-G., X.-Y. Li, H.-Z. Huang, and Y.-F. Li, "Fault prognosis of engineered systems: A deep learning perspective," *2019 Annual Reliability and Maintainability Symposium (RAMS)*, 1–7, 2019.
26. Merity, S., N. S. Keskar, and R. Socher, "Regularizing and optimizing LSTM language models," *International Conference on Learning Representations*, 2018.
27. Chen, J., H. Jing, Y. Chang, and Q. Liu, "Gated recurrent unit based recurrent neural network for remaining useful life prediction of nonlinear deterioration process," *Reliab. Eng. Syst. Saf.*, Vol. 185, 372–382, 2019.

28. Srivastava, N., G. Hinton, A. Krizhevsky, I. Sutskever, and R. Salakhutdinov, "Dropout: A simple way to prevent neural networks from overfitting," *J. Mach. Learn. Res.*, Vol. 15, No. 1, 1929–1958, 2014.
29. Zhang, Y., R. Xiong, H. He, and M. G. Pecht, "Long short-term memory recurrent neural network for remaining useful life prediction of lithium-ion batteries," *IEEE Trans. Veh. Technol.*, Vol. 67, No. 7, 5695–5705, 2018.
30. Kulkarni, C. S., J. R. Celaya, G. Biswas, and K. Goebel, "Prognostics of power electronics, methods and validation experiments," *2012 IEEE AUTOTESTCON Proceedings*, 194–199, 2012.
31. Kulkarni, C., G. Biswas, X. Koutsoukos, J. Celaya, and K. Goebel, "Integrated diagnostic/prognostic experimental setup for capacitor degradation and health monitoring," *2010 IEEE AUTOTESTCON*, 1–7, 2010.
32. Shatnawi, A., G. Al-Bdour, R. Al-Qurran, and M. Al-Ayyoub, "A comparative study of open source deep learning frameworks," *2018 9th International Conference on Information and Communication Systems (ICICS)*, 72–77, 2018.